



Exploring the Effects of Nonstationary and Diverse Covariates on Extreme Hot Events

ARTICLE INFO

Article Type
Original Research

Authors

Sedigheh Anvari, Ph.D.^{1*}
Mahnoosh Moghaddasi, Ph.D.^{2,3}

How to cite this article

Anvari S., Moghaddasi M. Exploring the Effects of Nonstationary and Diverse Covariates on Extreme Hot Events. ECOPERSIA 2023;11(4): 275-289

DOI:

20.1001.1.23222700.2023.11.3.1.5

¹ Assistant Professor, Department of Ecology, Institute of Science and High Technology and Environmental Science, Graduate University of Advanced Technology, Kerman, Iran.

² Associate professor, Department of Water Science and Engineering, Faculty of Agriculture and Environment, Arak University, Arak, Iran.

³ Research Institute for Water Science and Engineering, Arak University, Arak, Iran

* Correspondence

Address: Graduate University of Advanced Technology, Kerman, Iran.

Postal Code: 7631133131
Phone: +98 (34) 33776611
Fax: +98 (34) 33776617
Email: anvari.t@gmail.com

Article History

Received: September 22, 2023
Accepted: December 9, 2023
Published: December 20, 2023

ABSTRACT

Aims: Over the past twenty years, Iran has experienced a rise in extreme temperatures, particularly in hot events like extreme temperatures, as indicated by recent studies. This research seeks to analyze the annual maximum temperatures (AMT) in the dry Province of Kerman, Iran, focusing on both stationary (S) and nonstationary (NS) behavior.

Materials & Methods: Trend, homogeneity, and stationarity tests were utilized to identify the critical characteristics of the AMTs from 1979 to 2019. Frequency analysis of the AMTs was conducted using both stationary Generalized Extreme Value (S-GEV) and nonstationary GEV (NS-GEV) models, estimating distribution parameters through a maximum likelihood estimator (MLE). In addition to the time-varying NS-GEV (TNS-GEV) investigations, soil moisture (SM) was incorporated as a covariate.

Findings: Results demonstrate that, compared to the S-GEV case, the NS-GEV frequency analyses significantly impact the return values of the AMTs, leading to an increase. The NS-GEV estimations for 50-year return levels were significantly higher than those in the S-GEV. The study's findings revealed that the average Akaike Information Criterion (AIC) for both the S-GEV and TNS-GEV estimations decreased from 110 to 71 across all 12 selected stations in Kerman Province. The AIC value for the NS-GEV with the soil moisture (SM) covariate was approximately 94. Thus, the TNS-GEV frequency analysis of AMTs resulted in improved AIC values compared to the NS-GEV with soil moisture as the covariate.

Conclusion: Given the nonstationary (NS) conditions caused by natural and/or human activities, it is recommended to utilize NS frequency analysis for estimating hydrologic variables across different design periods. It has been noted that NS-GEV frequency analyses lead to higher return levels of AMTs than S-GEV analyses.

Keywords: Stationary/Nonstationary; Extreme temperature; GEV; Soil moisture covariate Frequency analysis; Kerman.

CITATION LINKS

[1] IPCC. Glossary of terms in managing the ris ... [2] Anvari S., Moghaddasi M. Historical Change ... [3] Westra S., Alexander L.V., Zwiers F. W. Glo ... [4] Donat M., Alexander L., Yang H., Durre I., ... [5] Andreadis K.M., Lettenmaier D.P. Trends in ... [6] Spinoni J., Naumann G., Vogt J.V. Pan-Europ ... [7] Moghaddasi M., Anvari S., Akhondi N. A trad ... [8] Anvari S., Moghaddasi M., Bagheri M.H. Drou ... [9] Razmi A., Golian S., Zahmatkesh Z. Nonstati ... [10] Berghuijs W.R., Allen S.T., Harrigan S., Ki ... [11] Archfield S.A., Hirsch R.M., Viglione A., B ... [12] Coles S., Bawa J., Trenner L., Dorazio P. A ... [13] Katz R.W., Parlange M.B., Naveau P. Statist ... [14] Hawkes P.J., Gonzalez-Marco D., Sánchez-Arc ... [15] AghaKouchak A., Nasrollahi N. Semi-parametr ... [16] Li L., Zhang L., Xia J., Gippel C. J., Wang ... [17] Katz R. Statistics of extremes in climate c ... [18] Vanem E. Nonstationary extreme value models ... [19] Miralles D.G., Teuling A.J., Van Heerwaarde ... [20] Ghavidel, R. Y., Rezaee, M., & Farajzadeh, ... [21] Hao Z., Hao F., Singh V.P., Ouyang W. Quant ... [22] Ganeshi N. G., Mujumdar M., Krishnan Goswam ... [23] Jowkar L., Panahi F., Sadatinejad S., Shakiba ... [24] Delavar, S., Anvari, S., Najafzadeh, M., & ... [25] Aksu H. Nonstationary analysis of the extre ... [26] Zamani R., Berndtsson R. Evaluation of CMIP ... [27] Babaeian I., Karimian M., Modirian R. Mirza ... [28] Moghaddasi M., Anvari S., Mohammadi T. Comp ... [29] Salarjazi M., Ghorbani K., Mohammadi M., A ... [30] New M., Hulme M., Jones P. Representing twe ... [31] Mitchell T.D. Jones P.D. An improved method ... [32] Hersbach H., Bell B., Berrisford P., Hiraha ... [33] Hersbach H., deRosnay P., Bell B. Operation ... [34] Trenberth K.E., Paolino D.A. The Northern H ... [35] Banerjee A., Dolado J.J., Galbraith J.W., & ... [36] Kwiatkowski D., Phillips P.C., Schmidt P., ... [37] Kumar S., Merwade V., Kam J., Thurner K. St ... [38] Mann H.B. Nonparametric tests against trend ... [39] Kendall M.G. Rank Correlation Methods. New ... [40] Sen P.K. Estimates of the regression coeffi ... [41] Pettitt A.N. A nonparametric approach to th ... [42] Delgado J.M., Apel H., Merz B. Flood trends ... [43] Debele S.E., Bogdanowicz E., Strupczewski W ... [44] Efron B. Maximum Likelihood and Decision Th ... [45] Gilleland E., Ribatet M., Stephenson A.G. A ... [46] Gilleland E., Katz R.W. extRemes 2.0: an ex ... [47] Cheng L., Gilleland E., Heaton M.J., AghaKo ... [48] Akaike H. A new look at the statistical mod ... [49] Whan K., Zscheischler J., Orth R., Shongwe ... [50] Teuling A.J., Seneviratne SI Contrasting sp ... [51] Hohenegger C., Brockhaus P., Bretherton C. ... [52] Emmanouil S., Langousis A., Nikolopoulos E. ...

Introduction

Extreme weather events have become more common and severe due to global climate change, impacting human life worldwide. Different regions of the world have experienced different levels of warming in the global surface temperatures. The highest temperature values in the global annual surface averages have mostly occurred in the past 20 years^[1]. In these years, Iran has also experienced unprecedented extreme hot temperatures in various climatic regions. The annual maximum temperature (AMT) has increased over time, and its extremely hot temperature distribution has shown nonstationary (NS) behavior^[2].

Extreme Value Theory (EVT) is a statistical theory that deals with extreme events like tail events or values lying beyond the range of traditional observations. EVT describes the distribution of the most extreme values, either the highest or the lowest, in a data set. EVT has been applied in various fields to model and predict extreme events that may have severe impacts, such as heat waves, heavy rainfall^[3,4], droughts^[5,8], sea levels^[9], and floods^[10,11].

Extreme climate studies can be divided into two categories. One category is the extreme climate indices, which use fixed or percentile thresholds to measure the extremeness of climate events. The other category is the frequency analysis, which examines the distribution of extreme values^[2,12]. Two standard methods for analyzing extreme values (EV) are block maxima (BM) and the peaks-over-threshold (POT). These methods select the most extreme values from a data set based on different criteria. The probability distributions that fit these methods are the generalized extreme value (GEV) and the generalized Pareto distribution (GPD), respectively^[13,16].

The extreme value analysis (EVA) can be performed under both stationary (S)

and nonstationary (NS) assumptions. These assumptions reflect whether the characteristics of extreme events, such as their frequency and intensity, are constant or changing over time. In this regard, Maximum likelihood estimation (MLE) is a simple and widely used method for EVA studies. MLE is a statistical technique that finds the best-fitting probability distribution and its parameters for a given data set based on the likelihood function^[7,12,17,18]. In addition, the trend component for hydroclimate extremes under NS conditions can be incorporated into the GEV parameters (μ : location, σ : scale, and ξ : shape) as a function of time or other hydroclimate covariates. Soil moisture (SM) and near-surface temperature are examples of covariates that can be considered to establish a link between extreme temperature and land-atmosphere interactions^[19,24].

Some recent studies have investigated the issue of nonstationary (NS) extreme temperature using the GEV model with different covariates. For instance, the NS-GEV model was used to analyze the extreme temperature of north-central India (NCI) and evaluated the effect of long-term soil moisture changes from 1948 to 2014^[22]. The return levels of absolute extreme temperatures in 50 stations in Turkey were also calculated and examined in time, and the teleconnection patterns of AO and NAO were the possible trend drivers. These studies demonstrate the significance and usefulness of the NS-GEV model for analyzing and forecasting extreme temperature events under changing climatic conditions^[25].

Several studies have observed positive trends in Iran's extreme temperatures and related indices^[26,27]. For example, the EVT methods, such as block maxima (BM) and peaks-over-threshold (POT), were utilized to analyze the NS behavior of maximum monthly temperature in the Arak plain of Iran from 1901 to 2016^[28]. The return periods of

extremely hot temperatures were calculated using long-term data from 41 urban areas in Iran. The Generalized additive Models for Location, Scale, and Shape (GAMLSS) were applied to examine how the return period of 50 and 100 maximum temperatures changed over time and space. Results revealed that the maximum temperature time series showed significant nonstationarity in 83% of urban areas in Iran. The return levels of maximum temperature increased over time and space, indicating a warming trend in Iran^[29].

Iran has a complex and variable temperature behavior due to its arid and semi-arid location, diverse climates, and landscapes. This makes it challenging to cope with the effects of climate change. However, most of the previous studies on extreme temperature in Iran have been limited in scope and have yet to account for the effect of hydro-climate variability in the temporal extreme temperature distribution. Therefore, this study addresses this gap by examining the extremely hot temperature in Kerman Province, located in southeastern Iran, which

ranges from dry to humid climates. We apply S-GEV and NS-GEV distribution functions with time and soil moisture covariates to capture the spatiotemporal changes in extremely hot temperatures. Finally, we estimate the return levels and analyze the regional differences in extreme temperature.

Study Area and Datasets

Iran covers an area of 1,648,195 km² in West Asia, and its location is between 24–40°N latitude and 43–62°E longitude. The country has a diverse topography, with an average height of 5,137m above sea level. Furthermore, the climate varies across different regions of Iran. For example, the central Provinces like Kerman have very hot summers. The average daily temperature in July is more than 38°C. Kerman Province, the case study of this research, has a diverse climate ranging from arid to humid and from mountainous to coastal. The location of Kerman Province and its 12 selected weather stations are shown as follows (Figure 1). The datasets of current research are as follows:

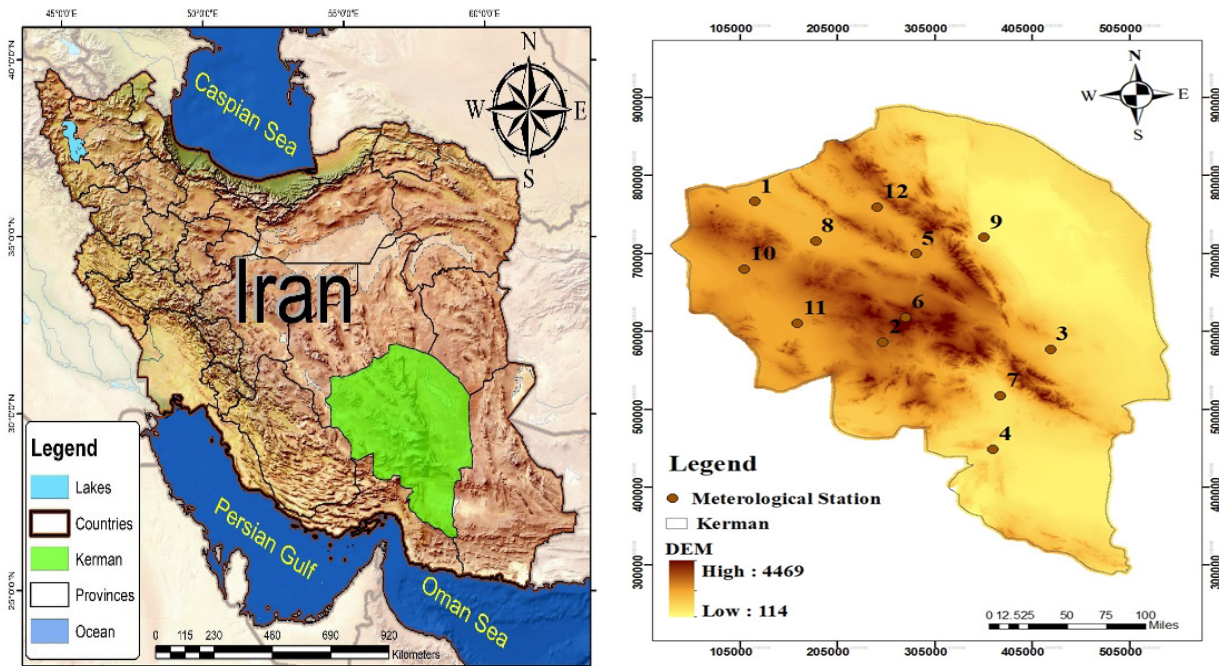


Figure 1) Geographic location of selected stations in Kerman Province, Iran [1. Anar, 2. Baft, 3. Bam, 4. Kahnooj, 5. Kerman, 6. Lalehzar, 7. Miandeh Jiroft, 8. Rafsanjan, 9. Shahdad, 10. Shahr Babak, 11. Sirjan, 12. Zarand].

Station-based observations: The monthly maximum temperature for 1979 to 2019 year for the 12 selected stations in Kerman Province was obtained from the official documents of the Iranian Ministry of Energy. These data were used to validate the maximum temperature data extracted from the CRU datasets. As illustrated (Figure 2), the boxplots of the maximum temperature (Tmax) time series for each of the 12 stations from 1979 to 2019.

As shown (Figure 2), boxplots with the median marked by the central line and the lower and upper edges represent the 25th and 75th percentiles, respectively. The whiskers extend to the most extreme non-outlier data points. Notably, the 75th percentiles in Bam, Kahnnoj, and Shahdad stations exceed 35, while Baft station recorded less than 30 °C. The boxplots also illustrate the variability of Tmax across stations and years and the presence of extreme values. Table 1 summarizes the statistical characteristics of the 41-year annual maximum temperatures (AMTs) extracted from CRU data for the selected stations.

– **CRU datasets** are produced by the Climatic Research Unit (CRU) at the University of East Anglia in the UK. They provide high-

resolution gridded datasets of various climate variables, such as temperature, precipitation, and cloud cover for all land areas at 0.5° resolution. The maximum temperature data on the monthly scale were downloaded for the 12 stations in Kerman Province from 1979 to 2019. These data were interpolated using the IDW method^[30,31]. The CRU data were then validated against the observed point-based data from the selected stations. To evaluate the accuracy of CRU data sets, the statistical criteria of coefficient of determination (R^2), normalized root mean square error (NRMSE), and mean bias error (MBE) have been employed. The results of these indices confirmed that the accuracy of the CRU data is reliable (Table 1).

– **ERA5 gridded datasets:** For all selected stations in this study, the monthly gridded datasets of soil moisture ($m^3.m^{-3}$) were obtained from ERA5(<https://www.ecmwf.int/en/forecasts/datasets/reanalysis-datasets/era5>) with a spatial resolution of 0.125° resolution for the period of 1979–2019. ERA5 is the latest global climate reanalysis produced by ECMWF(European Centre for Medium-Range Weather Forecasts), covering atmospheric conditions from January 1950 to the present. The ERA5 is the fifth generation

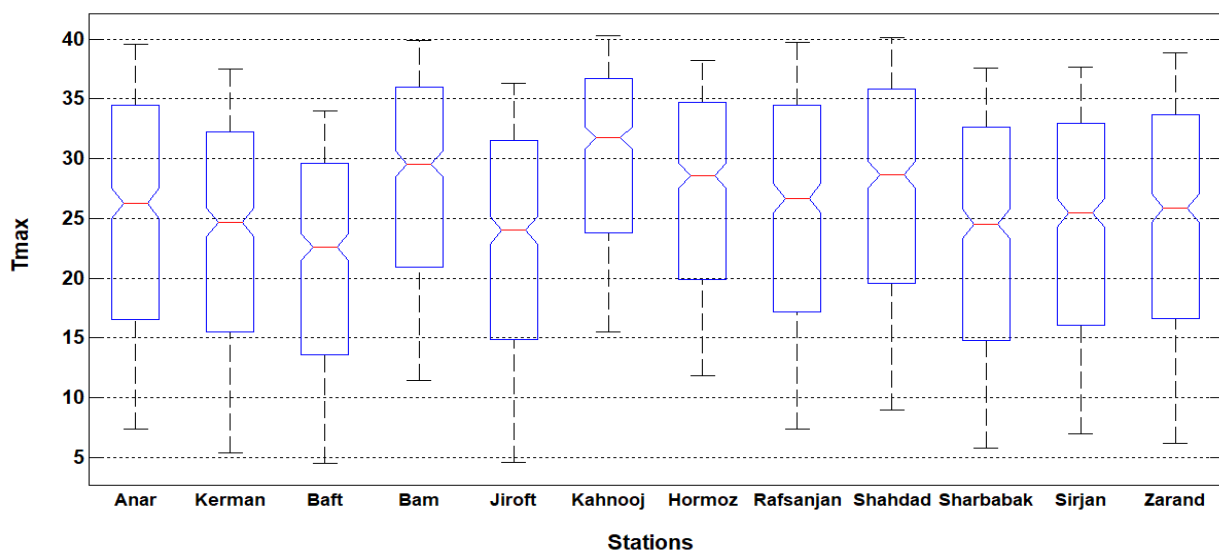


Figure 2) Boxplots of the Tmax time series for each of the 12 stations in Kerman Province.

Table 1) Summary statistics and quantiles of the CRU data for the selected stations.

Statistics	Baft	Rafsanjan	Kerman	Sirjan	Shahrabak	Zarand	Kahnoj	Bam	Jiroft	Shahdad	Anar
Num. data	41	41	41	41	41	41	41	41	41	41	41
Mean	38.37	37.73	35.53	36.04	35.94	36.83	38.60	38.37	34.59	38.41	37.84
St. deviation	0.82	0.95	0.91	0.84	0.88	0.96	0.76	0.82	0.91	0.93	0.93
Skewness	-0.05	-0.03	-0.10	-0.02	-0.03	-0.04	-0.08	-0.05	-0.20	-0.16	-0.15
Kurtosis	-0.67	-0.66	-0.60	-0.90	-0.90	-0.49	-0.26	-0.67	-0.78	-0.99	-0.83
10%quantile	37.5	36.4	34.4	34.9	34.7	35.6	37.5	37.5	33.3	37.2	36.5
25%quantile	37.7	36.9	34.7	35.2	35.2	36.1	38.1	37.7	34.0	37.7	37.1
50%quantile	38.3	37.9	35.7	36.1	36.1	37.0	38.6	38.3	34.8	38.6	38.0
75%quantile	39.0	38.3	36.2	36.6	36.5	37.5	39.1	39.0	35.2	39.1	38.4
90%quantile	39.4	38.9	36.6	37.0	37.0	37.9	39.5	39.4	35.7	39.6	39.0

ECMWF atmospheric global climate reanalysis produced by the Copernicus Climate Change Service (C3S) at ECMWF [32,33].

Methodology

This study followed a series of steps to analyze the historical changes in hot extreme temperatures about time and soil moisture covariates across the Kerman Province:

1. Data from station-based observations, CRU, and ERA5 were extracted for all 12 stations in the case study.
2. Nonparametric tests, including Mann-Kendall, ADF, and Pettit's test, were utilized to detect trends, stationarity, and homogeneity of the AMT, respectively.
3. The extreme distribution functions of S-GEV and NS-GEV were performed using the MLE method, examining the impact of time and SM covariates on the behavior of NS-GEV.
4. Frequency analysis was conducted to calculate the temperature values for different return periods.

Autocorrelation, homogeneity, trend, and stationarity tests

This section describes how we used some nonparametric tests to evaluate the quality of AMTs. The first step was to apply the outlier detection test to all AMT time series. Outliers in the extreme climatological data set can reveal necessary information

about the population. So, we determined the threshold value as $(Q3 + 3 \times IQR)$, where $Q3$ is the third quartile, and IQR is the interquartile range [34]. The time series randomness was also evaluated using the autocorrelation function, which measures the correlation between AMT values at different time lags to assess the dataset's time dependence. This study focused on the first-order autocorrelation coefficient, indicating the short-term memory of extremely hot temperatures.

In the following, the Mann-Kendall, ADF, and Pettit nonparametric tests were chosen to evaluate trends, stationarity, and homogeneity of AMTs. This selection is justified by their robustness, applicability to non-normally distributed data, and effectiveness in capturing non-linear patterns and abrupt changes. These tests provide valuable insights into extreme temperature time series' long-term behavior and characteristics, making them well-suited for rigorous statistical analysis in this context [35,37].

Mann-Kendall (MK) test and Sen's slope estimator: To detect any potential trends in the AMTs at a 95% confidence level, we used the nonparametric Mann-Kendall test [38,39] to identify potential trends in the AMTs.

This test effectively assesses changes in the median of a time series data over time. The MK test assumes that the null hypothesis (H_0) states the absence of a trend in the data time series. In contrast, the alternative hypothesis (H_1) suggests the presence of a trend. The following relationships were employed:

$$s = \sum_{i=1}^{n-1} \sum_{j=i+1}^n \text{sgn}(Y_j - Y_i) \quad \text{Eq. (1)}$$

$$\text{sgn}(Y_j - Y_i) = \begin{cases} +1 & \text{if } (Y_j - Y_i) > 0 \\ 0 & \text{if } (Y_j - Y_i) = 0 \\ -1 & \text{if } (Y_j - Y_i) < 0 \end{cases} \quad \text{Eq. (2)}$$

$$\text{VAR}(s) = \frac{1}{18} [n(n-1)(2n+5) - \sum_{p=1}^q t_p(t_p-1)(2t_p+5)] \quad \text{Eq. (3)}$$

$$Z_m = \begin{cases} \frac{s-1}{\sqrt{\text{VAR}(s)}} & \text{if } s > 0 \\ 0 & \text{if } s = 0 \\ \frac{s+1}{\sqrt{\text{VAR}(s)}} & \text{if } s < 0 \end{cases} \quad \text{Eq. (4)}$$

The test statistic, denoted as Z_m , is determined based on the number of data points (n), the i^{th} and j^{th} observations (Y_i and Y_j), the number of clusters with more than two members (q), and the number of data in the p^{th} class (t_p). The null hypothesis (H_0) is rejected only if the test statistic significantly deviates from zero at a 5% significance level, which occurs when $|Z_m| > 1.96$, indicating the presence of a trend in the time series^[39].

Sen's slope estimator^[40] was employed to ascertain the extent of potential trends in the AMTs. This method calculates the slope (indicating the linear rate of change) and the intercept using the following formula:

$$\beta_n = \text{Median} \left[\frac{Y_j - Y_i}{j - i}; Y_j \neq Y_i, i < j = 1, 2, \dots, n \right] \quad \text{Eq. (5)}$$

Herein, Y_i and Y_j are the extreme hot temperature values for years i and j ,

respectively, and n is the number of data. **Stationarity and Homogeneity Tests:** This section employed the Augmented Dickey-Fuller (ADF) test to examine the stationarity of AMTs in all 12 selected stations at a 95% confidence level. The ADF test's null hypothesis (H_0) proposes that the time series is stationary, while the alternative hypothesis (H_1) suggests that the time series is not stationary (NS)^[35]. For further details on this test, refer to^[36]. We also utilized Pettitt's test^[41] to examine the homogeneity of the AMTs. This nonparametric test can identify any changes in the mean of the AMTs at an unknown time. It does not rely on any assumptions about the distribution of the time series. The H_0 is no change in the distribution of a random variable sequence; the H_1 is that the distribution function $F_1(x)$ of the random variables from X_1 to X_t is different from the distribution function $F_2(x)$ of the random variables from X_{t+1} to X_t . More details about this test can be found in^[41].

Generalized Extreme Value (GEV)

The flexibility of the GEV lies in its ability to model various extreme behaviors through the utilization of the three distribution parameters of (μ, σ, ξ) : (1) the location parameter (μ), which represents the central part of the distribution; (2) the scale parameter (σ), which defines the magnitude of deviation around the location parameter; and (3) the shape parameter (ξ), which governs the tail behavior of the GEV distribution^[17,42].

The GEV distribution unifies the type I (Gumbel with $\xi=0$), type II (Fréchet with $\xi>0$), and type III (Weibull with $\xi<0$) EV distributions into a single family, offering a continuous range of shapes. In essence, GEV is a three-parameter model that combines Gumbel, Fréchet, and Weibull distributions into one form^[12], as represented in Equation (6 and 7):

$$f(x) = p(X \leq x) = H(x; \xi, \sigma, \mu) \\ = \begin{cases} \exp\left(-\left(1 - \frac{\xi}{\sigma}(x - \mu)\right)^{1/\xi}\right) & \xi \neq 0 \\ e^{-\frac{x-\mu}{\sigma}} & \xi = 0 \end{cases} \quad \text{Eq. (6)}$$

$$F(x) = 1 - \frac{1}{T} \quad \text{Eq. (7)}$$

The shape parameter ξ is the Extreme Value Index (EVI), which determines the tail behavior of the GEV. For the Fréchet distribution ($\xi > 0$), the tail displays a power function decay, showing a heavy tail. Conversely, the reversed Weibull ($\xi < 0$) exhibits a tail with a finite right endpoint, signifying a bounded tail. In the case of Gumbel ($\xi = 0$), the tail decays exponentially, indicating a lighter tail. Coles [12] proposed the following distribution function for a nonstationary GEV with time-dependent parameters:

$$F(x; \mu(t), \sigma(t), \xi) = \exp\left\{-\left(1 + \frac{\xi}{\sigma(t)}(x - \mu(t))\right)^{\frac{1}{\xi}}\right\}$$

Eq. (8)

The parameter ξ is commonly assumed to be constant, as its estimation is highly uncertain, even in the stationary case, as noted by [43].

The Maximum Likelihood Estimation (MLE) Method

The MLE is a commonly employed method for fitting conceptual models and estimating the parameters of a Probability Density Function (PDF) [44]. To illustrate, let us consider evaluating a random variable X with the PDF $f(x; a_1, a_2, \dots, a_m)$ and parameters a_i , where $i = 1, 2, \dots, m$. In MLE, the first step involves extracting a random sample of data $x_1, x_2, \dots, x_3, \dots, x_n$ from this probability density, whose joint PDF is expressed as:

$$f(x_1, x_2, x_3, \dots, x_n; a_1, a_2, \dots, a_m) \\ = \prod_{i=1}^n f(x_i; a_1, a_2, a_3, \dots, a_m) \quad \text{Eq. (9)}$$

Here, the probability of achieving a given value of X (e.g., X_1) is proportional to $f(x; a_1, a_2, \dots, a_m)$. Similarly, the probability of obtaining the random sample $x_1, x_2, \dots, x_3, \dots, x_n$ from the population of X is proportional to the product of the individual or joint PDFs. This product is known as the likelihood function, which can be derived using Equation (10):

$$L = \prod_{i=1}^n f(x_i; a_1, a_2, a_3, \dots, a_m) \quad \text{Eq. (10)}$$

Here, a_i , $i = 1, 2, \dots, m$, represents the unknown parameters. By maximizing n random observations from $f(x_i; a_1, a_2, a_3, \dots, a_m)$, we obtain the likelihood of the sample. The parameter estimates resulting from this maximization are called Maximum Likelihood Estimates (MLEs). Since maximizing the log L is equivalent to maximizing L concerning the same values of a_i , an alternative representation of the maximum likelihood formula is as follows:

$$\ln L = L^* = \ln \prod_{i=1}^n f(x_i; a_1, a_2, a_3, \dots, a_m) \\ = \sum_{i=1}^n \ln f(x_i; a_1, a_2, a_3, \dots, a_m) \quad \text{Eq. (11)}$$

Numerous nonstationary (NS) EVA software tools are available for analyzing extreme hydro-climate data. For instance, the R-package "ismev" models the NS as a linear regression function of generic covariates [45]. Herein, we utilized the "extRemes" package that provides EVA capability and assesses the uncertainties of parameters [46]. Consequently, the NS model parameters were obtained using the MLE likelihood method with the "extRemes" package.

Time-varying NS-GEV (TNS-GEV) and NS-GEV with Soil Moisture Covariate

The NS-GEV distribution has parameters that depend on covariates, such as time or other physical drivers like soil moisture (SM). These covariates reflect the changes in the characteristics of extreme events over time or space [2,47].

To explore the link between AMTs and SM,

we computed the antecedent SM during the summer (May-June-July) and assessed its correlation with the AMTs from June to August (JJA). The NS-GEV distribution with time-varying parameters is described by Equation (12), while Equation (13) represents the NS-GEV equation with SM as a covariate.

$$\mu(t) = \mu_0 + \mu_1 t \quad \text{Eq. (12)}$$

$$\mu(\text{SM}) = \mu_0 + \mu_1 \text{SM} \quad \text{Eq. (13)}$$

where μ_0 and μ_1 are the S- and NS-location parameters, respectively. Finally, to compare the goodness of the fitted distributions, the Akaike Information Criterion (AIC) was employed [48].

Findings

Trend, Homogeneity, and Stationary Frequency Analysis of AMTs

In this section, the analysis for homogeneity revealed that all the AMT time series for the chosen stations exhibited breaks around

1996, roughly in the middle of the time series (Table 2). The homogeneity of the AMT time-series declined after this year. The overall disruption inhomogeneity of extreme temperatures was interpreted as an indication of climatic change across the study area.

The Mann–Kendall test was employed to check the significance of the trend in AMTs at the 5% significance level for the selected stations. The results illustrated that the computed p-value was smaller than 0.05 for all 12 stations. It means we can reject the null hypothesis(H0) of no trend and accept the alternative hypothesis(H1) of a significant trend. Based on the temperature analysis in the selected stations, it was concluded that all stations have recorded higher increasing trends(Figure 3).

Once the trend in the AMTs was confirmed, the Augmented Dickey–Fuller (ADF) test [35] was applied to assess data stationarity. The ADF results indicated that AMT time series in

Table 2) Statistical test results of homogeneity, trend, and stationarity for 12 selected stations in Kerman Province(R1: *First-lag autocorrelation, *Trend detected).

Climate Region	Station Name	R1	Homogeneous	Possible Break		Trend		Sen's Slope	Stationary	
				Year	Trend	Kendall's Tau	P-Value		Stationary	ADF Test
Excessively-Arid	Anar	*	No	1996	*	0.6552	0.000	0.064	No	-3.256
Mediterranean	Baft	*	No	1996	*	0.5920	0.000	0.055	No	-2.630
Excessively-Arid	Bam	*	No	1996	*	0.6024	0.000	0.056	No	-3.197
Arid	Kahnooj	*	No	1996	*	0.4939	0.000	0.049	No	-3.441
Arid	Kerman	*	No	1996	*	0.6115	0.000	0.063	No	-2.890
Arid	Lalehzar	*	No	1996	*	0.6016	0.000	0.056	No	-2.790
Excessively-Arid	Miandeh Jiroft	*	No	1996	*	0.6370	0.000	0.064	No	-3.089
Excessively-Arid	Rafsanjan	*	No	1996	*	0.6353	0.000	0.067	No	-3.152
Arid	Shahdad	*	No	1996	*	0.6197	0.000	0.063	No	-3.088
Excessively-Arid	Shahr Babak	*	No	1996	*	0.6519	0.000	0.062	No	-3.101
Excessively-Arid	Sirjan	*	No	1996	*	0.6329	0.000	0.060	No	-2.975
Arid	Zarand	*	No	1996	*	0.6304	0.000	0.066	No	-3.063

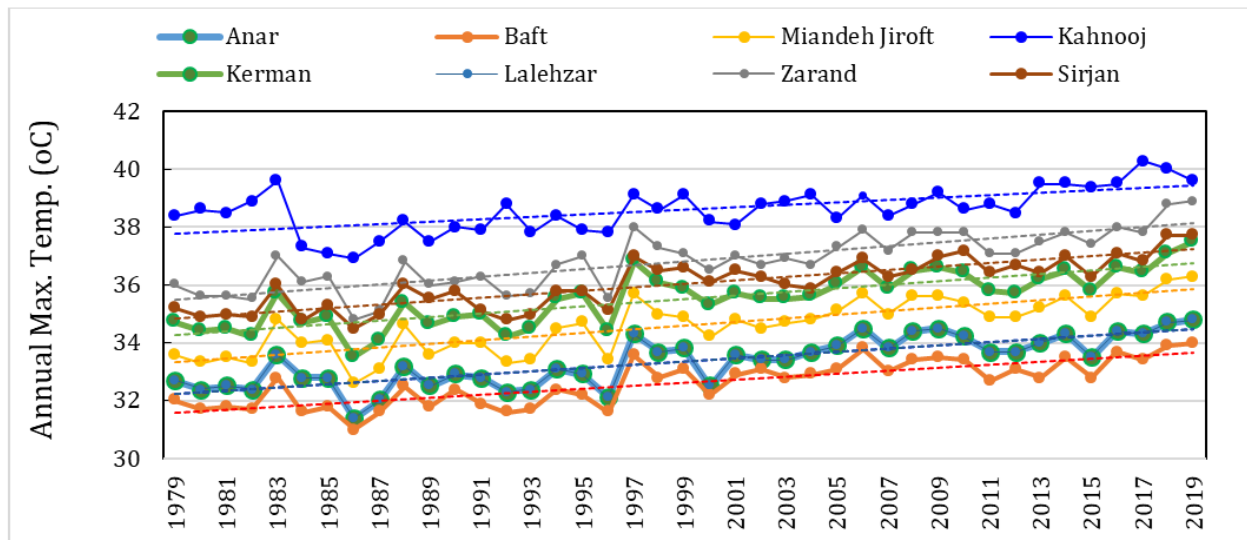


Figure 3) Time series of Annual Maximum Temperature for some selected stations.

all 12 selected stations were nonstationary (NS). For example, at the Bam station, the ADF statistic was -3.197, lower than the critical value of -3.401. Additionally, the *p*-value exceeded the 5% significance level, concluding that the null hypothesis of the NS state should be accepted.

Figures 4 and 5 show the results of fitting the standard S-GEV model to the Kerman and Bam stations' annual maximum temperatures (AMTs). The first graph in these figures is the quantile-quantile (Q-Q) plot that compares the empirical and theoretical quantiles of AMTs under the GEV assumption. The second graph in these figures is the return level plot that shows the relationship between the return levels and return periods of AMTs. These plots indicate a good agreement between the GEV model and the AMT data. As shown (Figures 4 and 5), for the 50-year return level, the S-GEV model resulted in extreme temperatures equaling 39.86°C and 37.27°C with a 95% confidence interval of [39,46,40,26] and [36,83,37,69], for Bam and Kerman stations, respectively. The AIC indices for stationary assumptions were equal to 105 and 114, respectively. The results showed that all the mentioned stations have a nonstationary trend.

This issue was also confirmed by Moghaddasi et al. [28] for another region of Iran dominated by an arid climate zone. Aksu (2021) also approved that over the fifty stations extracted from seven geographical regions of Turkey, more than half of the absolute annual maximum time series (26/50) showed a nonstationary positive trend [25].

Discussion

The AIC for S-GEV and NS-GEV were equal to 113.96 and 73.96 at Kerman station, showing a significant decrease in these indices, indicating that the NS behavior of AMT is acceptable. The AIC of other stations also confirmed this behavior. As an example, the TNS-GEV for the Kerman station resulted in Equation (14):

$$\mu(t) = 0.063 * t + 35.23 \quad \text{Eq. (14)}$$

In the following, the NS-GEV frequency analysis of AMT about the SM variable as a covariate was considered during the 1979–2019 period. To this end, the relationship between AMT-JJA and SM-MJJ was investigated for all the selected stations at the mentioned period. For instance, a significant negative correlation coefficient

was observed in Kerman station, equal to 0.81. This negative correlation was also compatible with Whan et al.'s [49]. For Southern-Central and Southeastern Europe, these researchers applied GEV distribution to investigate the influence of soil moisture (SM) as the covariate on extreme temperatures in summer (TX_x). They identified a negative relationship between SM and TX_x , where a 100 mm decrease in model-based SM is associated with a 1.6°C increase in TX_x in their case study. As shown (Table 3), the AIC criteria for three S-GEV, TNS-GEV, and NS-GEN models with SM as a covariate at the selected stations. Regarding the NS-GEV with SM-MJJ as the covariate, the AIC was equal to 71.62 for the Kerman station, but according to Table 3, the AIC under SM-MJJ was mostly bigger than AIC under TNS-GEV in other stations. In other words, the SM-MJJ as a covariate can be used only in Kerman station. As previously noted, we used the NS-GEV

model to analyze the frequency of AMTs from 1979 to 2019 using time and soil moisture (SM) covariates. SM significantly impacts water and energy cycles and temperature extremes by modifying the soil's thermal properties, surface albedo, precipitation, and evapotranspiration processes [50,51]. Therefore, we utilized SM as a suitable covariate for the NS-GEV model to investigate future hot extremes, potential droughts, and time. Our results demonstrated that the interactions between AMTs and SM varied across different climatic zones of Kerman Province. Although we assumed a linear relationship between AMTs and SM in this study, this assumption increases the estimation variance [52], which can be considered a limitation of this work.

Conclusion

Annual maximum temperature (AMT) affects heatstroke, energy use, cooling systems, water demand, and heart health. Climate change may alter how often it gets very hot in

Table 3) The AIC criteria for three GEV models with SM as a covariate at the selected stations.

Station	S-GEV	TNS-GEV	NS-GEV-SM
Anar	114.659	72.836	106.224
Baft	99.185	59.722	91.377
Bam	105.167	71.348	71.328
Kahnooj	100.431	77.325	94.930
Kerman	113.966	73.959	71.629
Lalehzar	105.162	69.424	98.375
Miandeh Jiroft	112.872	72.168	94.558
Rafsanjan	117.695	76.838	111.256
Shahdad	114.072	74.189	115.238
Shahr Babak	110.685	66.759	89.913
Sirjan	106.869	58.938	96.825
Zarand	118.748	76.383	83.229

fevd(x = ASTmax, data = A, type = "GEV", method = "MLE", units = "degc")

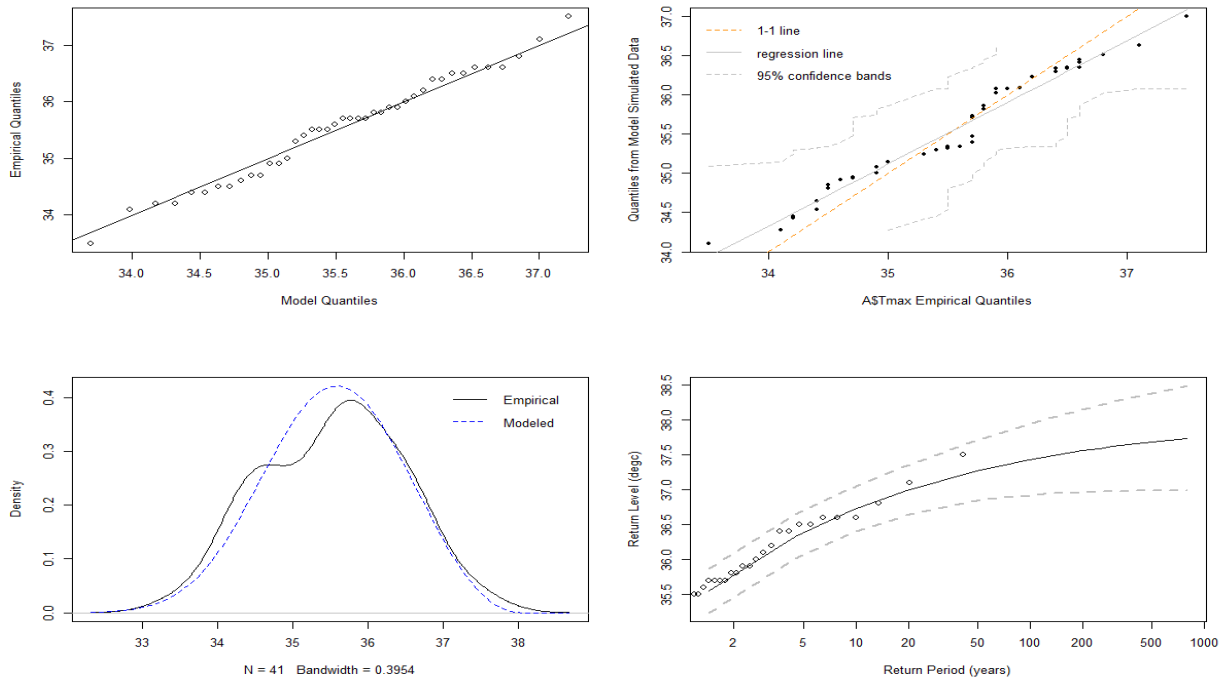


Figure 4) The return level against the return period for Kerman station.

fevd(x = ASTmax, data = A, type = "GEV", method = "MLE", units = "degc")

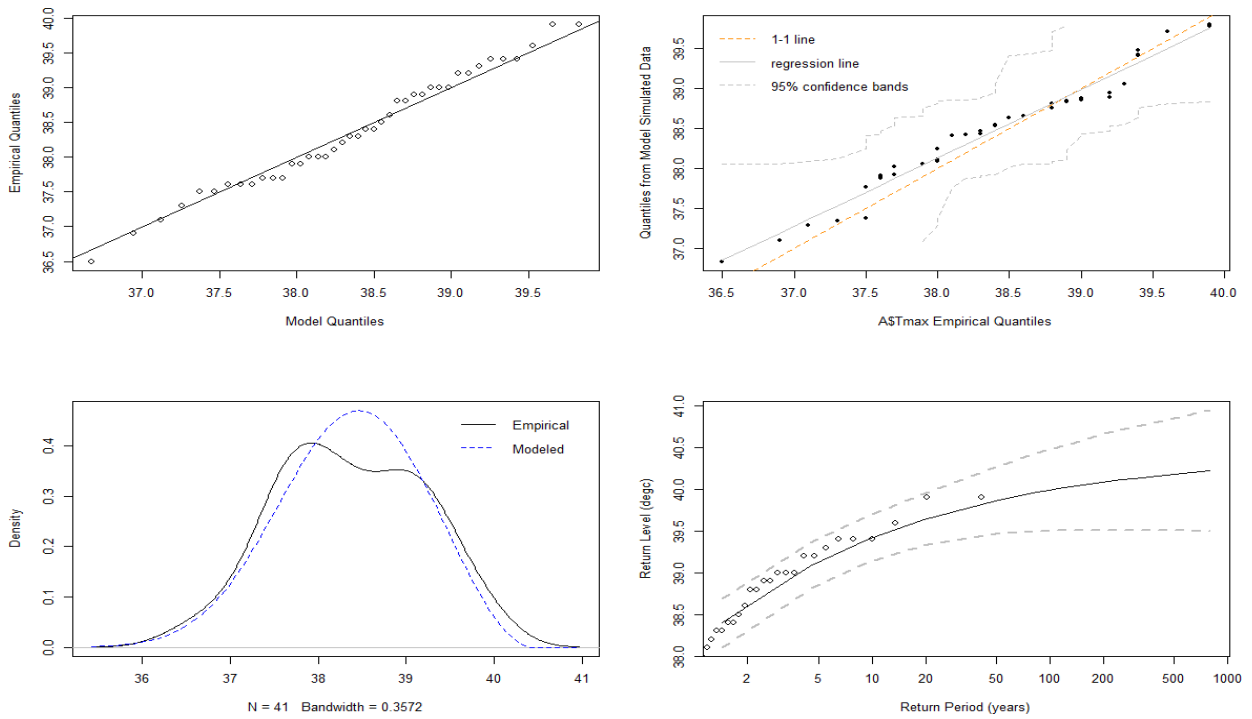


Figure 5) The return level against the return period for Bam station.

a year. In the present study, the stationary (S) and nonstationary (NS) generalized extreme value (GEV) distribution functions were fitted to AMTs derived from 12 weather stations in Kerman Province during the 1979–2019 period. The required AMTs for this period were extracted from the CRU gridded data sets, and the soil moisture (SM) data was collected from ERA5. The parameters of the S-GEV and NS-GEV distributions were estimated using the MLE method.

Moreover, the akaike information criterion (AIC) was employed to identify the most appropriate S- and NS-GEV distribution functions. Considering the Augmented Dickey-Fuller (ADF) results, it was concluded that the AMT time series was NS. This result was also confirmed by AIC criteria calculated for both S-GEV and NS-GEV assumptions. The time-varying NS-GEV (TNS-GEV) frequency analyses were carried out for all 12 stations in Kerman Province. As a result, the NS behavior of AMTs for the selected stations was found to be affected by the covariates of time. Also, a negative correlation was observed between AMTs and antecedent SM in the summer season (SM-MJJ), which was above 0.5 for all stations. Furthermore, the NS-GEV frequency analysis of AMTs with SM-MJJ as the covariate resulted only in better AIC values at the Kerman station.

The results of our study on the changing patterns of extreme hot temperature, the link between soil moisture and extreme temperature, and the rising trend of extreme temperature are consistent with the findings of previous research by Whan et al. (2015), Aksu (2021), and Moghaddasi et al. (2022). The NS-GEV model used SM as a covariate to assess potential interactions with future hot extremes in this study. SM, a random variable varying in time and space, was assumed to have a linear relationship with AMTs, which can increase estimation variance. This limitation should be recognized in future

studies. Extreme temperature trends also have multifaceted implications for local communities, agriculture, and other relevant sectors. Vulnerable populations, such as the elderly and those with pre-existing health conditions, may face heightened health risks. Furthermore, extreme temperatures can strain infrastructure, potentially leading to power outages and increased demand for cooling systems. Agriculture is also at risk, as heat stress can impact crop yields and livestock productivity, with potential economic and food security implications for local and global markets.

Given the nonstationary (NS) conditions of extreme temperatures resulting from natural and/or human activities, applying NS frequency analysis for estimating hydrological variables across different design periods is recommended. Furthermore, this study emphasizes the importance of considering soil moisture (SM) as a crucial factor in predicting future extreme heat events. It also underscores the necessity for further investigation into the non-linear relationship between SM and extreme temperatures and the role of prior drought in heightening extreme heat events. These findings carry significant implications for climate change adaptation and mitigation efforts, as well as for developing effective strategies to manage the impacts of extreme heat events. Due to the nonstationary nature of drought propagation in changing environments, providing precise drought warnings is challenging. The practical goal of this research is to mitigate the impact of drought and climate change.

Acknowledgments

The authors gratefully acknowledge the support from the Graduate University of Advanced Technology (Institute of Science and High Technology and Environmental Science) (No. 1401/3022) for this research work.

Ethical permission: The authors certify that their work is entirely original and that any use of the work or words of others has been appropriately cited or quoted.

Authors' contributions: [Sedigheh Anvari] and [Mahnoosh Moghaddasi] were responsible for material preparation, data collection, and analysis. [Sedigheh Anvari] drafted the initial manuscript and handled reviewer responses. The final manuscript was reviewed and approved by both [Sedigheh Anvari] and [Mahnoosh Moghaddasi]

Funding/Support: This research was supported by the Graduate University of Advanced Technology, and the authors are grateful for this support.

Conflict of interest: The authors have no conflicts of interest to declare regarding the publication of this article. They confirm that all co-authors have consented to and are fully aware of the submission.

References

1. IPCC. Glossary of terms in managing the risks of extreme events and disasters to advance climate change adaptation. Field C.B., Barros V., Stocker T.F., Qin D., Dokken D.J., Ebi K.L., Midgley P.M. A Special Report of Working Groups I and II of the Intergovernmental Panel on Climate Change (IPCC). Cambridge University Press, Cambridge, UK, and New York, NY, USA, 2012; 555-564.
2. Anvari S., Moghaddasi M. Historical Changes of Extreme Temperature in relation to Soil Moisture over Different Climatic Zones of Iran. *Stoch. Env. Res. Risk Asses.* 2023;1(1):1-17.
3. Westra S., Alexander L.V., Zwieters F. W. Global increasing trends in annual maximum daily precipitation. *J. clim.*2013;26(11):3904-3918.
4. Donat M., Alexander L., Yang H., Durre I., Vose R., Dunn R., Willett K., Aguilar E., Brunet M., Caesar J., Hewitson B., Jack C., Klein Tank A. M. G., Kruger A. C., Marengo J., Peterson T. C., Renom M., Oria Rojas C., Rusticucci M., Salinger J., Elrayah A. S., Sekele S. S., Srivastava A. K., Trewin B., Villarreal C., Vincent L. A., Zhai P., Zhang X., Kitching S. Updated analyses of temperature and precipitation extreme indices since the beginning of the twentieth century: The HadEX2 dataset. *J. Geophys. Res. Atmos.* 2013; 118(5): 2098-2118.
5. Andreadis K.M., Lettenmaier D.P. Trends in 20th century drought over the continental United States. *Geophys. Res. Lett.* 2006; 33(10).
6. Spinoni J., Naumann G., Vogt J.V. Pan-European seasonal trends and recent changes of drought frequency and severity, *Global Planet. Change.* 2017;148(1):113-130.
7. Moghaddasi M., Anvari S., Akhondi N. A trade-off analysis of adaptive and non-adaptive future optimized rule curves based on simulation algorithm and hedging rules. *Theor. Appl. Climato.*2022;148(1):65-78.
8. Anvari S., Moghaddasi M., Bagheri M.H. Drought mitigation through a hedging-based model of reservoir-farm systems considering climate and streamflow variations. *Theor. Appl. Climato.* 2023;152(1-2):723-737.
9. Razmi A., Golian S., Zahmatkesh Z. Nonstationary frequency analysis of extreme water level: application of annual maximum series and peak-over threshold approaches. *Water Resour. Manag.* 2017; 31(7): 2065-2083.
10. Berghuijs W.R., Allen S.T., Harrigan S., Kirchner J.W. Growing spatial scales of synchronous river flooding in Europe. *Geophys. Res. Lett.* 2019a: 46(3): 1423-1428.
11. Archfield S.A., Hirsch R.M., Viglione A., Blöschl G. Fragmented patterns of flood change across the United States. *Geophys. Res. Lett.* 2016; 43(19): 10-232.
12. Coles S., Bawa J., Trenner L., Dorazio P. An introduction to statistical modeling of extreme values. London: Springer; 2001:208p.
13. Katz R.W., Parlange M.B., Naveau P. Statistics of extremes in hydrology. *Adv. Water. Resour.* 2002; 25(8-12): 1287-1304.
14. Hawkes P.J., Gonzalez-Marco D., Sánchez-Arcilla A., Prinos P. Best practice for the estimation of extremes: A review. *J. Hydraul. Res.* 2008; 46(S2):324-332.
15. AghaKouchak A., Nasrollahi N. Semi-parametric and parametric inference of extreme value models for rainfall data. *Water. Resour. Manag.* 2010; 24:1229-1249.
16. Li L., Zhang L., Xia J., Gippel C. J., Wang R., Zeng S. Implications of modelled climate and land cover changes on runoff in the middle route of the south to north water transfer project in China. *Water Resour. Manag.* 2015; 29(8): 2563-2579.
17. Katz R. Statistics of extremes in climate change. *Clim. Change.* 2010; 100(1):71-76.
18. Vanem E. Nonstationary extreme value models to account for trends and shifts in the extreme wave climate due to climate change. *Appl. Ocean. Res.* 2015; 52(1): 201-211.
19. Miralles D.G., Teuling A.J., Van Heerwaarden, C.C., Vilà-Guerau J. Mega-heatwave temperatures due to combined soil desiccation and atmospheric heat accumulation. *Nat. Geosci.* 2014; 7(5): 345-349.

20. Ghavidel, R. Y., Rezaee, M., & Farajzadeh, A. M. (2016). The Application of Normalized Temperature Deviation (NTD) for Identification and Synoptic analysis of high extreme temperatures in south-east region of Iran. *ECOPERSIA* 2016, 19(4): 123-140.
21. Hao Z., Hao F., Singh V.P., Ouyang W. Quantitative risk assessment of the effects of drought on extreme temperature in eastern China. *J. Geophys. Res-Atmos.* 2017; 122(17): 9050-9059.
22. Ganeshi N. G., Mujumdar M., Krishnan Goswami R.M. Understanding the linkage between soil moisture variability and temperature extremes over the Indian region. *J. Hydrol.* 2020; 589: 125183.
23. Jowkar L, Panahi F, Sadatinejad A. The Spatio-Temporal Variability of Extreme Temperature Using Gridded AgMERRA Dataset over the Bakhtegan-Maharloo Basin, Iran. *ECOPERSIA* 2021; 9(3):179-189.
24. Delavar S., Anvari S., Najafzadeh M., Fathian, F. A Review of Stationary and Non-Stationary Indices for Drought Monitoring in Iran and other Countries. *Irrig. Water. Eng.* (2023).
25. Aksu H. Nonstationary analysis of the extreme temperatures in Turkey. *Dynam. Atmos. Ocean.* 2021; 95:101238.
26. Zamani R., Berndtsson R. Evaluation of CMIP5 models for west and southwest Iran using TOPSISI-based method. *Theor. Appl. Climato.* 2018; 137(1): 533-543.
27. Babaeian I., Karimian M., Modirian R. Mirzaei E. Future climate change projection over Iran using CMIP5 data during 2020-2100. *NIVAR.* 2019: 43(104-105): 61-70.
28. Moghaddasi M., Anvari S., Mohammadi T. Comparison of extreme value theory approaches in temperature frequency analysis (case study: Arak plain in Iran). *Arab. J. Geosci.* 2022; 15(12):1-13.
29. Salarijazi M., Ghorbani K., Mohammadi M., Ahmadianfar I., Mohammadrezapour O., Naser M.H., and Yaseen Z.M. Spatial-temporal estimation of maximum temperature high returns periods for annual time series considering stationary/nonstationary approaches for Iran urban area. *Urban. Climate*, 2023; 49: 101504.
30. New M., Hulme M., Jones P. Representing twentieth-century space-time climate variability. Part I: Development of a 1961-90 mean monthly terrestrial climatology. *J. Climate.* 1999; 12(3):829-856.
31. Mitchell T.D. Jones P.D. An improved method of constructing a database of monthly climate observations and associated high-resolution grids. *Int J Climatol.* 2005; 25(6): 693-712.
32. Hersbach H., Bell B., Berrisford P., Hirahara S., Horányi, A., Muñoz-Sabater J., Thépaut J.N. The ERA5 global reanalysis. *Q. J. Roy. Meteor. Soc.* 2020; 146(730): 1999-2049.
33. Hersbach H., deRosnay P., Bell B. Operational global reanalysis: progress, future directions and synergies with NWP, ERA. Report. Series. 2018; 27, ECMWF, Reading, UK.
34. Trenberth K.E., Paolino D.A. The Northern Hemisphere sea-level pressure data set: trends, errors, and discontinuities. *Mon. Wea. Rev.* 1980; 108(7): 856-872.
35. Banerjee A., Dolado J.J., Galbraith J.W., Hendry D. Co-integration, Error Correction, and the Econometric Analysis of nonstationary Data. Oxford University Press, 1993.
36. Kwiatkowski D., Phillips P.C., Schmidt P., & Shin Y. Testing the null hypothesis of stationarity against the alternative of a unit root: How sure are we that economic time series have a unit root? *J. Econom.* 1992; 54(1-3): 159-178.
37. Kumar S., Merwade V., Kam J., Thurner K. Stream flow trends in Indiana: Effects of long-term persistence, precipitation, and subsurface drains. *J. Hydrol.* 2009; 374(1-2):171-183.
38. Mann H.B. Nonparametric tests against trend. *J. Econom.* 1945; 13(1): 245-259.
39. Kendall M.G. Rank Correlation Methods. New York, NY: Oxford University Press. 1975:272p.
40. Sen P.K. Estimates of the regression coefficient based on Kendall's Tau. *J. Am. Stat. Assoc.* 1968; 63(324):1379-1389.
41. Pettitt A.N. A nonparametric approach to the change point problem. *J. R. Stat. Soc. Ser. C. (Appl. Stat.)* 1979; 28(2): 126-135.
42. Delgado J.M., Apel H., Merz B. Flood trends and variability in the Mekong river. *Hydrol. Earth. Syst. Sci.* 2010; 14(3): 407-418.
43. Debele S.E., Bogdanowicz E., Strupczewski W.G. Around and about an application of the GAMLSS package to nonstationary flood frequency analysis. *Acta. Geophys.* 2017; 65(1): 885-892.
44. Efron B. Maximum Likelihood and Decision Theory. *Ann. Stat.* 1982; 10(2): 340- 356.
45. Gilleland E., Ribatet M., Stephenson A.G. A software review for extreme value analysis. *Extremes (Boston).* 2013; 16(1): 103-119.
46. Gilleland E., Katz R.W. extRemes 2.0: an extreme value analysis package in R. *J. Stat. Softw.* 2016; 72 (8): 1-39.
47. Cheng L., Gilleland E., Heaton M.J., AghaKouchak A. Empirical Bayes estimation for the conditional extreme value model. *Stat.* 2014; 3(1), 391-406.
48. Akaike H. A new look at the statistical model identification. *IEEE. Trans. Automat. Contr.* 1974; 19(6): 716-723.
49. Whan K., Zscheischler J., Orth R., Shongwe M., Rahimi M., Asare, E.O. Seneviratne SI Impact of soil moisture on extreme maximum temperatures in

- Europe. *Weather Clim. Extremes*. 2015; 9(1):57-67.
50. Teuling A.J, Seneviratne SI Contrasting spectral changes limit albedo impact on land-atmosphere coupling during the 2003 European heat wave. *Geophys. Res. Lett.* 2008; 35(3).
51. Hohenegger C., Brockhaus P., Bretherton C. S., Schär C. The soil moisture–precipitation feedback in simulations with explicit and parameterized convection. *J. Climate*. 2009; 22(19): 5003-5020.
52. Emmanouil S., Langousis A., Nikolopoulos E.I., Anagnostou EN The Spatiotemporal Evolution of Rainfall Extremes in a Changing Climate: A CONUS-Wide Assessment Based on Multifractal Scaling Arguments. *Earths. Future*. 2022; 10(3): e2021EF002539.